RESEARCH ARTICLE

Global Change Biology WILEY

Soil carbon stocks in stable tropical landforms are dominated by geochemical controls and not by land use

Mario Reichenbach[1] | Peter Fiener[1] | Alison Hoyt[2,3] | Susan Trumbore[2] | Johan Six[4] | Sebastian Doetterl[1,4]

[1]Institute of Geography, Augsburg University, Augsburg, Germany

[2]Department of Biogeochemical Processes, Max Planck Institute for Biogeochemistry, Jena, Germany

[3]Department of Earth System Science, Stanford University, Stanford, California, USA

[4]Department of Environmental Systems Science, ETH Zurich, Zurich, Switzerland

Correspondence
Mario Reichenbach, Augsburg University, Alter Postweg 118, 86159 Augsburg, Germany.
Email: mario.reichenbach@geo.uni-augsburg.de

Sebastian Doetterl, Institute of Geography, Augsburg University, Augsburg 86159, Germany.
Email: sdoetterl@usys.ethz.ch

Funding information
Deutsche Forschungsgemeinschaft, Grant/Award Number: 387472333

Abstract

Soil organic carbon (SOC) dynamics depend on soil properties derived from the geo-climatic conditions under which soils develop and are in many cases modified by land conversion. However, SOC stabilization and the responses of SOC to land use change are not well constrained in deeply weathered tropical soils, which are dominated by less reactive minerals than those in temperate regions. Along a gradient of geochemically distinct soil parent materials, we investigated differences in SOC stocks and SOC (Δ^{14}C) turnover time across soil profile depth between montane tropical forest and cropland situated on flat, non-erosive plateau landforms. We show that SOC stocks and soil Δ^{14}C patterns do not differ significantly with land use, but that differences in SOC can be explained by the physicochemical properties of soils. More specifically, labile organo-mineral associations in combination with exchangeable base cations were identified as the dominating controls over soil C stocks and turnover. We argue that due to their long weathering history, the investigated tropical soils do not provide enough reactive minerals for the stabilization of C input in either high input (tropical forest) or low-input (cropland) systems. Since these soils exceeded their maximum potential for the mineral related stabilization of SOC, potential positive effects of reforestation on tropical SOC storage are most likely limited to minor differences in topsoil without major impacts on subsoil C stocks. Hence, in deeply weathered soils, increasing C inputs may lead to the accumulation of a larger readily available SOC pool, but does not contribute to long-term SOC stabilization.

KEYWORDS
SOC stabilization, SOC turnover, soil carbon dynamics, tropical biogeochemistry, tropical land conversion, tropical soils

1 | INTRODUCTION

The loss of forests driven by cropland expansion and deforestation for timber, agriculture, or charcoal production is a global problem, with great consequences for terrestrial carbon cycling. The vast majority of research analyzing the effect of land conversion on SOC dynamics focuses on geochemically less altered and more intensively managed soils of the temperate zone (Cotrufo et al., 2019; Degryze et al., 2004; Gregorich et al., 1998; Lugato et al., 2018). In these younger, often more productive soils of the temperate zone, land conversion from forest to cropland accelerates SOC decomposition by enhancing biological activity (e.g., by changing

soil moisture, aeration, and temperature), paired with lower C inputs from plant primary productivity and the removal of biomass through harvesting. Studies on the effects of land conversion on SOC dynamics in geochemically more altered soils in low intensity management systems of the Tropics, however, are still rare (Köchy et al., 2015; Schimel et al., 2015), despite their importance for the global C cycle and high rates of deforestation (Amundson et al., 2015; Curtis et al., 2018; Gerland et al., 2014; Tyukavina et al., 2018). The consequences of this accelerated land conversion for biogeochemical cycles are unclear, particularly for tropical Africa. Limited observations of processes controlling SOC dynamics in critical regions of the African Tropics with growing land pressure lead to substantial uncertainties in predicting SOC stocks after conversion and limit our ability to upscale local experimental findings to larger scales (Sanderman & Chappell, 2013; Vereecken et al., 2016; von Fromm et al., 2021). Thus, land use change effects on soils remain poorly constrained for Africa, despite their importance (Cusack et al., 2013; Don et al., 2011; Kirsten et al., 2021; Perrin et al., 2014).

Previous studies show that tropical land conversion from forest to cropland may drive substantial SOC losses just as observed in temperate zones (Don et al., 2011). According to the literature, most tropical soils lose between 30% and 70% of SOC during the first few years after conversion from forest to cropland (Don et al., 2011; Gregorich et al., 1998; Guillaume et al., 2015; Wei et al., 2014). These SOC losses are not limited to topsoil and the loss of labile C sources alone, but are also detectable in subsoil where C is predominately sorbed to and stabilized by minerals (Don et al., 2011; Luo et al., 2020). Despite these reported general trends, presumed SOC losses upon conversion to cropland are difficult to predict across larger scales. Data are often derived from regions under seasonal climate or geomorphologically and geologically active zones where soils are generally younger and less weathered. Additionally, SOC dynamics depend on several interacting factors like mineralogy, crop and soil types, management practices, and land use history (Don et al., 2011; Fujisaki et al., 2015). The combination of these factors is usually not assessed across regions, catchments, or even fields. Recent studies do indicate that substantial variability in the potential of tropical soils to stabilize C is more governed by geochemical properties (i.e., pedogenic metal phases, clay mineralogy, texture) derived from its soil parent material (Doetterl, Asifiwe, et al., 2021; Reichenbach et al., 2021), as well as the degree of soil weathering (Kirsten et al., 2021) than by land use (von Fromm et al., 2021).

In mineral soils, the dominant long-term C stabilization mechanism is the sorption of functional C groups to mineral surfaces (Dick et al., 2005; Herold et al., 2014; Kramer et al., 2012; Lawrence et al., 2015). However, the quantity of secondary, pedogenic minerals is not always indicative of better C stabilization (Bruun et al., 2010; McNally et al., 2017; Rasmussen et al., 2018). Instead, mineralogical properties of the soil parent material and its weathering stage govern long-term C stabilization (Heckman et al., 2009). Due to their environmental boundary conditions and their extensive weathering history, most tropical soils are dominated by end member minerals such as 1:1 clays (e.g., kaolinite) as well as highly crystalline Fe oxyhydroxides and Fe oxides, which have a lower potential for the sorption of organic matter (Barré et al., 2014; Doetterl et al., 2018; Ito & Wagai, 2017; Six, Conant, et al., 2002). Thus, the reduced mineral reactivity of tropical soils (Doetterl et al., 2018; Mendez et al., 2022) compared to temperate soils leads to a lower potential to store C despite higher inputs in natural (tropical forest) ecosystems.

In this study, we aimed to analyze and understand the effect of geochemical properties and weathering status of soil parent material on SOC stocks and soil C turnover time following land conversion from tropical forest to subsistence cropland in tropical central Africa. We postulated that geochemical properties of parent material and the weathering status of soils govern SOC loss and soil C turnover time following conversion from forest to cropland. More specifically, we hypothesized that deeply weathered and less reactive soils would be less responsive to changes in C input when C inputs exceed the capacity of soils to store C. Consequently, tropical SOC dynamics may be less sensitive to land use change and be more governed by soil geochemistry.

2 | MATERIALS AND METHODS

2.1 | Study region—Geoclimatic characterization

This study is embedded in the larger framework of project TropSOC (Doetterl, Asifiwe, et al., 2021; Doetterl, Bukombe, et al., 2021) which aims to study the effects of soil geochemistry, weathering and erosion on tropical forest, and cropland C cycles. Our study sites are located along the Albertine Rift, a part of the East African Rift System in the border region between the Democratic Republic of the Congo (DRC), Rwanda and Uganda (Figure 1). The region was chosen due to its large variety of soil parent material (geological units), while the environmental conditions are similar. The region is characterized by tropical humid climate (Köppen Af-Am) with monsoonal dynamics. The regional climate is subdivided into four seasons (weak dry in December–February; strong rains in March–May; strong dry in June–August; and weak rains in September–November) each covering three months (Bukombe et al., 2022; Doetterl, Asifiwe, et al., 2021). The mean annual temperature (MAT) varies between 15.3 and 19.2°C and mean annual precipitation (MAP) varies between 1697 and 1924 mm (Fick & Hijmans, 2017). In general, MAP is higher in study sites under forest compared to cropland. MAT and PET are slightly higher in the study sites under cropland compared to forest, at least in the mafic and mixed study regions (Table 1).

Soils in DRC are developed from mafic magmatic rocks and are classified as alic Nitisols (ochric), alic Nitisols (vetic), and mollic Nitisols (ochric; Doetterl, Asifiwe, et al., 2021); this region is further called *mafic* region. Soils in Uganda are developed from felsic magmatic and metamorphic rocks: they are classified as sederalic Nitisols (ochric), haplic Lixisols (nitic), and luvic Nitisols (endogleyic; Doetterl, Asifiwe, et al., 2021) and this region is further called *felsic* region. Since the region is tectonically active, re-fertilization of
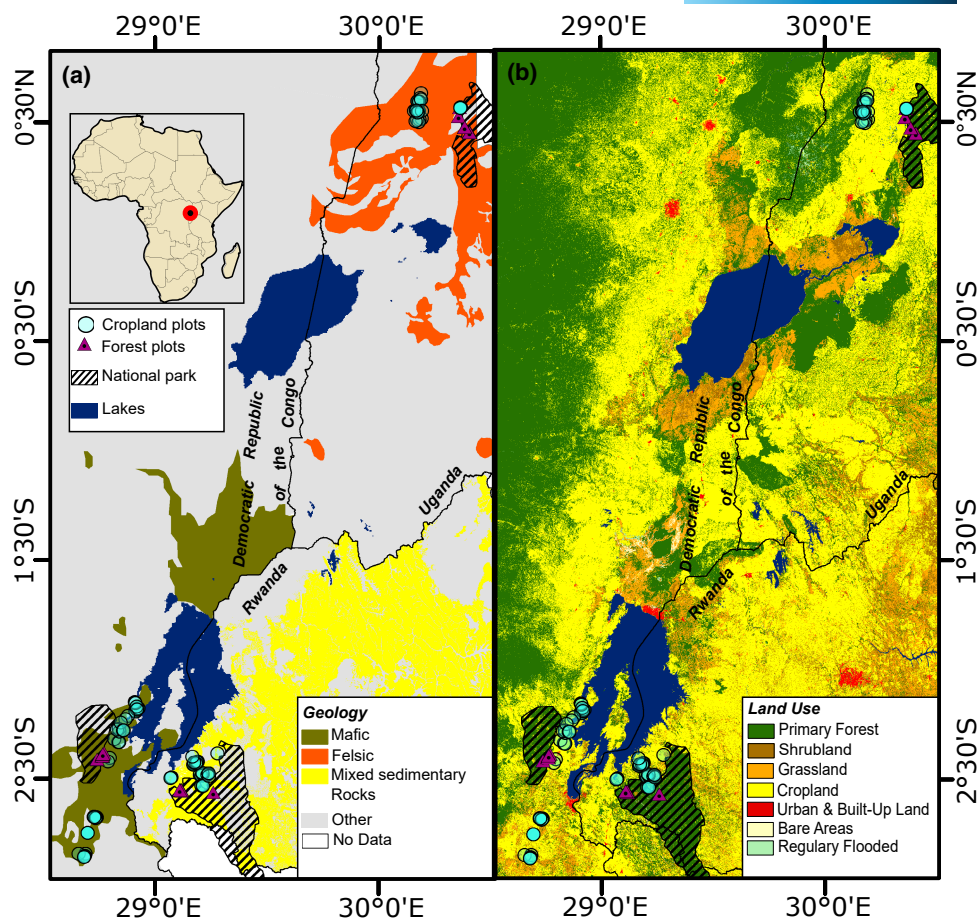
FIGURE 1 Overview of the study region with respect to (a) geology and (b) land use (modified from Doetterl, Asifiwe, et al., 2021) with line features delineating national parks.

TABLE 1 Climatic parameters for land uses within test regions. Data show mean and standard deviation and are compiled from the WorlClim 2 database (Fick & Hijmans, 2017).

	MAT (°C)	MAP (mm year^{-1})	PET (mm year^{-1})
Mafic			
Forest	15.5 ± 0.3	1928 ± 3	1124 ± 16
Cropland	18.2 ± 0.7	1606 ± 88	1303 ± 80
Felsic			
Forest	19.2 ± 0	1697 ± 0	1486 ± 0
Cropland	18.9 ± 0.3	1465 ± 13	1371 ± 20
Mixed sedimentary			
Forest	17.3 ± 0.1	1691 ± 0	1242 ± 8
Cropland	18.2 ± 0.2	1499 ± 46	1296 ± 25

Abbreviations: MAP, mean annual precipitation; MAT, mean annual temperature; PET, potential evapotranspiration.

soils with rock-derived nutrients by pyroclastica occurs to various degrees at a local scale (Bailey et al., 2005; Barker & Nixon, 1989; Eby et al., 2009). Study sites in Rwanda consist of mixed sedimentary rocks dominated by quartz-rich sandstone and schists and the

soils are classified as haplic Acrisols (nitic), acric Ferralsols (vetic), and acric Ferralsols (gleyic; Doetterl, Asifiwe, et al., 2021). This region is further called *mixed sedimentary* region. A specific feature of soils in this region is the presence of fossil, geogenic organic carbon free of radiocarbon in the parent material (dark clay-silt schists). For further details on the soil mineralogy of the study region, please refer to Bukombe et al. (2021, 2022), Doetterl, Asifiwe, et al. (2021) and Reichenbach et al. (2021).

2.2 | Study region—Land use and vegetation

The dominant natural vegetation in the area is tropical montane forest (Bukombe et al., 2022; Doetterl, Asifiwe, et al., 2021). Based on available information, all forest stands within our study sites are >300-year-old growth forests (Besnard et al., 2021). For most of the surrounding area, however, this natural vegetation did undergo a rapid conversion to cropland during recent decades (Gerland et al., 2014; Tyukavina et al., 2018). Today, most of the area is dominated by low-input, hand-hoed cropland managed by subsistence farmers (Figure 1; Dewitte et al., 2013; Dressée & Lepersonne, 1949; Friedl et al., 2013; Verdoodt & Van

Ranst, 2003). Local agriculture is characterized by rotations of cassava and maize, as well as various legumes and vegetables with little to no fertilizer input (Mangaza et al., 2021; Ordway et al., 2017; Tyukavina et al., 2018).

Before analyzing our soil data, we assessed potential differences in the time since land conversion from forest to cropland in our study sites, to determine its potential influence on SOC stocks. To understand the history of land conversion throughout the study regions, historical satellite images (1985–2022) based on Landsat 4–8 satellite data providing multi-band surface reflectance properties were analyzed using the Google Earth Engine time-lapse function (Gorelick et al., 2017). The results of the satellite data analyses were additionally evaluated through farmer questionnaires collected in 2018–2020 (Doetterl, Asifiwe, et al., 2021) where we acquired information on the time since deforestation. This analysis revealed that all cropland sites in this study area were converted before 1985. Other studies have found that the largest effects on SOC dynamics occur in the first three decades after conversion (Don et al., 2011; Guillaume et al., 2015). Thus, we concluded that differences in conversion timing were unlikely to impact our results, as all cropland sites should have had sufficient and similar amounts of time for SOC stocks to equilibrate to the new land use and land cover.

2.3 | Study design and soil sampling

A total of 29 study sites were established consisting of eight forest sites (two to three replicates in each geochemical region) and 21 cropland sites (five to nine replicates in each geochemical region). Forest study sites within each geochemical region were established within $40 \times 40\,m$ plots following an international, standardized protocol for tropical forest analysis (Marthews et al., 2014). Cropland study sites were established within $3 \times 3\,m$ plots cultivated with cassava only. Only study sites located on morphodynamically stable plateau positions were considered in this study to exclude the effect of soil redistribution with soil losses through erosion on slopes and soil gains through deposition in valleys after conversion of natural forest to cropland. Within each study site, four soil cores from forest and two soil cores from cropland were taken and combined to one depth-explicit composite sample representing one study site. Leaf litter (L horizon) and organic soil material (O horizon) were removed prior to drilling. Cores were taken using percussion drilling and soil column sampling equipment allowing for undisturbed sampling of 1 m deep soil cores at 9 cm diameter. Soil bulk density samples were taken with Kopecky cylinders of known volume ($98.13\,cm^3$) or derived from the known volume and weight of the soils sampled by percussion drilling. From the eight forest and 21 cropland sites, we overall produced 29 composite soil cores (to 1 m soil depth), which were subdivided in 10 cm depth increments. As some drillings could not reach 1 m soil depth, this resulted in 282 samples for analysis. Please refer to Doetterl, Asifiwe, et al. (2021) for a more detailed description of the study and sampling design.

2.4 | Soil analysis

As this study is part of an extensive sampling and analysis campaign of project TropSOC, previous work has analyzed a wide range of soil physical and chemical properties that are published in a project-specific database (Doetterl, Asifiwe, et al., 2021, Doetterl, Bukombe, et al., 2021), where details of the methods used are described. Therefore, we only provide a brief overview of the analytical methods in the following sections. Importantly, for sample analyses, a two-step approach was followed. First, 20% of all soil samples in project TropSOC covering a wide range of geoclimatic as well as geochemical conditions and land uses were analyzed based on classical wet chemistry methods. These were then used to calibrate a spectroscopic database (Summerauer et al., 2021).

2.4.1 | Key reference methods

Soil bulk density samples were oven-dried at 105°C for 24 h and weighed subsequently. Note that rock content (>2 mm) of all samples was negligible due to the generally deep weathering and long, relatively undisturbed period of soil development (Doetterl, Asifiwe, et al., 2021, Doetterl, Bukombe, et al., 2021). Soil texture (clay, silt, sand) was analyzed using the Bouyoucos hydrometer method (Bouyoucos, 1962) modified following Beretta et al. (2014).

A three-step sequential extraction scheme of Al, Fe, and Mn bearing pedogenic organo-mineral associations and oxyhydroxides (Stucki et al., 1988) was performed in the following order: (1) Extraction with sodium pyrophosphate at pH 10 following procedures by Bascomb (1968), (2) Extraction with ammonium oxalate-oxalic acid at pH 3 following Dahlgren (1994) and (3) Extraction with dithionite–citrate–bicarbonate (DCB) at pH 8 following Mehra and Jackson (1960). All extracts, including the calibration standards, were filtered through a grade 41 Whatman filter and diluted (1:1000) prior to analysis on the inductively coupled plasma optical emission spectrometry (ICP-OES; 5100 ICP-OES Agilent Technologies). In our sequential extraction of pedogenic metal phases, the pyrophosphate extraction was assumed to primarily retrieve Al, Fe, Mn from dissolution of labile organo-metal complexes and associations but may dissolve some non-crystalline short-range order (SRO) minerals and/or promote limited dispersion of ferrihydrite and goethite colloids. It is therefore more accurate to interpret them as both organo-mineral nanoparticles and organo-metal complexes (pyrophosphate extractable complexes ($\sum$Al, Fe, Mn); Rennert, 2019). The oxalate extraction of residual soil (following the pyrophosphate extraction) is interpreted to retrieve Al, Fe, and Mn from the complete dissolution of non-crystalline SRO minerals and ferrihydrite that form more stable organo-mineral complexes (oxalate extractable complexes ($\sum$Al, Fe, Mn)). It is also assumed that the oxalate extraction partially dissolves magnetite, hematite, and gibbsite (Rennert, 2019). The DCB method is interpreted to release highly crystalline forms of Al, Fe, and Mn from the complete dissolution of ferrihydrite, and goethite as well as partial dissolution of hematite, magnetite, and

gibbsite (DCB extractable complexes ($\sum$Al, Fe, Mn); Rennert, 2019) that showed no strong role for the stabilization of C in soil (Mikutta et al., 2009). However, recent studies in a tropical context document C accumulation with larger amounts of DCB extractable oxides, but did not employ sequential extraction as performed in our study (Kirsten et al., 2021).

Total elemental composition was determined by ICP-OES for analyzing calcium (Ca), magnesium (Mg), sodium (Na), potassium (K), phosphorous (P), aluminum (Al), iron (Fe), and manganese (Mn). One gram of powdered sample material was placed in digestion tubes and boiled for 90 min at 120°C in aqua regia (2 mL bi-distilled water, 2 mL 70% nitric acid (HNO_3), 6 mL 37% hydrochloric acid (HCl)) using a DigiPREP digestion system (DigiPREP MS SCP Science, Canada). All extracts, including the calibration standards, were filtered through a grade 41 Whatman filter and diluted with a ratio of 1:2 for Ca, Mg, Na, K, P, and 1:1000 for A, Fe, Mn using a dilution system (Hamilton 100). All extracted elements (aqua regia, sequential oxide extraction) are reported by mass.

Soil pH (KCl) was determined potentiometrically with a glass electrode using a portable multiparameter (Meter HI9828, Hanna Instruments US Inc.) following the protocol by Black (1965) on 20g of 2mm sieved bulk soil samples. Plant available P was analyzed on 2mm sieved bulk soil using the Bray 2 method (Okalebo et al., 2002). Exchangeable bases were measured on 2mm sieved bulk soil by percolation with $BaCl_2$ at pH 8.1. The percolate was then analyzed via flame photometry and atomic absorption spectrophotometry (Pauwels et al., 1992).

Total carbon (TC) and total nitrogen (TN) were analyzed using dry combustion (Vario EL Cube CNS Elementar Analyzer, Germany) with the C:N ratio used as an indicator for soil organic matter (SOM) quality. None of the samples showed any reaction when treated with 10% HCl and thus all C and N sources were considered of organic nature. SOC stocks of the bulk soil were calculated by multiplying the SOC concentration by soil bulk density and the thickness of the depth increment (10 cm). Please note that we focused on mineral C stocks and excluded C stocks from litter and organic soil horizons from forest to ensure comparability with cropland soils. Bulk soil Δ^{14}C was analyzed for selected depth increments (0–10, 30–40, 60–70cm) on graphite prepared from purified CO_2 released on combustion (Steinhof et al., 2017) using AMS (accelerator mass spectrometry) at the Max Planck Institute for Biogeochemistry (Jena, Germany) and are reported using the conventions of Stuiver and Polach (1977).

2.4.2 | Soil spectroscopy

All values for the presented variables (Table 2) have been analyzed using a Bruker Vertex 70, near and mid-infrared (NIR-MIR) Fourier transform FT-IR spectrometer (Doetterl, Asifiwe, et al., 2021) following the workflow of Summerauer et al. (2021). Please note that the intercept calculated in the predictive regression models is not forced through zero. Therefore, predicted values based on

low calibration values near zero can result in slightly negative values due to the uncertainty of the predictive model. We tested if statistical outcomes would differ when using the dataset including negative values from the dataset using zeros. The results and conclusions did not change and thus we decided to set all negative values to zero since negative elemental contents do not exist in nature. NIR-MIR predictions resulted in high to very high performance in explaining the observed variability (R^2 = .69–.93) for all assessed values, except for soil bulk density (R^2 = .43; Table 2). Thus, we used the soil bulk density derived from Kopecky cylinders instead of FT-IR spectrometry derived values to calculate SOC stocks.

2.5 | Statistical data analysis

2.5.1 | Standardization and cluster analyses

In a first step, prior to all statistical analyses, (except for analysis of variances (ANOVAs)), due to the differences in units and ranges of the target and predictor variables, Z-score standardization was applied to increase the comparability of effect sizes between predictors following Lacrose (2004). In a second step, (unrotated) principal component analysis (PCA) and cluster analysis using K-means partitioning clustering were performed to structure the dataset based on (geo)chemical characteristics with relation to fertility and mineralogy derived from soil parent material. Our reasoning for this choice is that tropical plant growth can be limited by rock-derived nutrients, that can be partly depleted in deeply weathered tropical soils (Augusto et al., 2017; Vitousek et al., 2010). Similarly, mineral C stabilization in tropical soils is often directly or indirectly driven by its pedogenic metal content because chemical soil weathering of primary minerals results in the formation of minerals that can sorb C (Reichenbach et al., 2021; von Fromm et al., 2021). Thus, we interpret the sum of total Al, Fe, and Mn (metals ($\sum$total Al, Fe, Mn)) as a proxy for soil mineral C stabilization (PC 2, Figure 2). To limit the effects of biological disturbance (root growth, bioturbation etc.) on the assessed geochemical—parent material derived—soil variables, we considered only deeper subsoil samples for the cluster analyses (70–80, 80–90, and 90–100cm; n = 82). Cluster analysis was realized using the R-package *Factoextra* (Kassambara & Mundt, 2020) following Han et al. (2012).

2.5.2 | Comparing mean values/ANOVA analyses

In a third step, depth-explicit patterns of SOC stocks and soil Δ^{14}C were assessed across both land use types and the identified geochemical clusters (see Section 3.1) using one-way ANOVA analyses (Crawley, 2009). Differences across geochemical clusters and land use for SOC variables (SOC stock, soil Δ^{14}C) were assessed by testing for equality of means. Please note that the study design resulted in a larger sample size of cropland sites than forest sites, varying group

TABLE 2 Soil property calibrations with near- and mid-infrared spectroscopy (Summerauer et al., 2021).

Parameter	Unit	Mid-infrared spectroscopy prediction		Sample size	Reference method	References
		R^2	RMSE			
SOC variables						
SOC	wt%	.92	0.53	282	Dry combustion	Nelson and Sommers (1996)
Soil Δ^{14}C	‰	.69	103.54	282	Elementar Analyzer coupled to an IRMS, AMS spectrometer	Stuiver and Polach (1977)
Soil organic matter (SOM) quality						
C:N	—	.84	11.73	282	Dry combustion	Nelson and Sommers (1996)
Soil physical variables						
Bulk density	g cm^{-3}	.43	0.27	282	Kopecky cylinder	Blake and Hartge (1986)
Clay	%	.93	4.43	282	Bouyoucos hydrometer	Bouyoucos (1962)
Silt	%	.80	4.02	282	Bouyoucos hydrometer	Bouyoucos (1962)
Sand	%	.90	5.28	282	Bouyoucos hydrometer	Bouyoucos (1962)
Mineral C stabilization potential						
Pyro. extr. oxides (Al, Fe, Mn)	wt%	.71	0.08	282	Three-step sequential extraction	Stucki et al. (1988)
Oxalate extr. oxides (Al, Fe, Mn)	wt%	.66	0.30	282	Three-step sequential extraction	Stucki et al. (1988)
DCB extr. oxides (Al, Fe, Mn)	wt%	.93	0.34	282	Three-step sequential extraction	Stucki et al. (1988)
Metals (∑total Al, Fe, Mn)	wt%	.88	0.45	282	ICP-OES	Hossner (1996)
Soil fertility						
Soil pH (KCl)	—	.87	0.27	282	Potentiometrically with a glass electrode	Black (1965)
Bray-P	mg kg^{-1}	.81	29.96	282	Bray 2	Okalebo et al. (2002)
Total P	wt%	.74	0.06	282	ICP-OES	Hossner (1996)
Exchangeable bases cations	meq 100 g^{-1}	.72	0.81	282	Flame photometry and AAS spectrophotometry	Pauwels et al. (1992)
TRB (∑total Ca, Mg, K, Na)	wt%	.73	2.00	282	ICP-OES	Hossner (1996)

Abbreviations: ANOVA, analysis of variance; DCB extr. oxides (∑Al, Fe, Mn), dithionite–citrate–bicarbonate extractable oxides of Al, Fe, and Mn; oxalate extr. oxides (∑Al, Fe, Mn), oxalate extractable oxides of Al, Fe, and Mn; pyro. extr. complexes (∑Al, Fe, Mn), pyrophosphate extractable organo-mineral complexes of Al, Fe, and Mn; VIF, variation inflation factor.

sizes (n = 7–21 per group with generally more cropland than forest plots within groups), as well as varying distances between cropland sites compared to forest sites of the same group. Thus, standard deviations of groups with cropland plots are generally larger than those of groups with little to no cropland. Therefore, before performing any mean value comparison, we conducted Levene's test to avoid type I error in ANOVA caused by heteroscedasticity (Moder, 2007). Based on the outcome, either one-way ANOVA (equal variances) or Welch-statistic (unequal variances) was used. Similarly, to compare the means of multiple groups, post-hoc testing was applied either with Bonferroni correction (equal variances) or Tamhane T2 (unequal variances) based on the outcome of the Levene's test (Day & Quinn, 1989).

2.5.3 | Regression analyses and minimizing multicollinearity effects

Stepwise linear regression analyses were used to build depth-explicit prediction models for SOC stocks and soil Δ^{14}C. An overview of ranges of soil properties considered for regression analyses is given in Table 3. To minimize multicollinearity effects and to prevent overfitting in the regression analysis, we assessed the variation inflation factor (VIF) for our model structures before analyzing model outcomes, starting with nine geochemical variables and samples stemming from all investigated geochemical clusters and land uses (n = 282; Table S1). After calculating the VIF for each run, the geochemical variable with the highest

TABLE 3 Ranges of soil properties in each geochemical cluster including samples from all soil depths (0–100 cm).

	Parameter	Unit	Used for regression	Low fertility/low stabilization potential Min–Max	n	Low fertility/high stabilization potential Min–Max	n	High fertility/low stabilization potential Min–Max	n
Target	SOC variables								
	SOC	t C ha^{-1}	Yes	1.1–62.0	125	0.0–66.0	90	4.0–64.0	67
	Soil $\Delta^{14}C$	‰	Yes	−477.5–160.9	125	−437.6–152.3	90	−512.4–119.1	67
Explanatory	Soil organic matter (SOM) quality								
	C:N	—	No	1.8–35.5	125	0.0–30.7	90	0.0–34.3	67
	Texture								
	Clay	%	Yes	21.9–82.6	125	26.5–83.9	90	13.9–46.1	67
	Silt	%	Yes	1.6–22.2	125	2.6–15.8	90	8.3–25.7	67
	Sand	%	No	8.4–65.2	125	13.5–52.4	90	39.8–65.7	67
	Mineral C stabilization potential								
	Pyro. extr. oxides (Al, Fe, Mn)	wt%	Yes	0.0–1.4	125	0.0–1.1	90	0.1–0.8	67
	Oxalate extr. oxides (Al, Fe, Mn)	wt%	Yes	0.0–2.3	125	1.0–4.0	90	0.7–4.5	67
	DCB extr. oxides (Al, Fe, Mn)	wt%	No	1.0–12.1	125	9.1–17.7	90	0.0–8.0	67
	Metals ($\sum$total Al, Fe, Mn)	wt%	No	4.1–18.8	125	16.0–27.1	90	3.5–14.3	67
	Soil fertility								
	Soil pH (KCl)	—	No	3.2–6.2	125	2.8–4.8	90	4.4–6.4	67
	Bray-P	mg kg^{-1}	No	0.0–78.2	125	0.0–30.7	90	47.0–300.6	67
	Total P	wt%	No	0.0–0.2	125	0.1–0.3	90	0.2–0.7	67
	Exchangeable bases (Ca, Mg, K)	meq 100 g^{-1}	Yes	0.0–23.8	125	0.0–12.0	90	6.0–27.9	67
	TRB	wt%	No	0.0–0.9	125	0.1–0.8	90	0.9–2.1	67

VIF and the lowest correlation (Pearson r) with SOC variables was excluded iteratively until the VIF of each of the remaining variables was <2.5 (Senaviratna & Cooray, 2019). Pearson correlation was used to assess the cross-correlation between retained and removed variables (Figure S1). Thus, a subset of geochemical variables was created that can be used as covariates in the prediction models without losing information from the initial dataset. The following variables remained after four runs of the VIF assessment: The sum of pyrophosphate extractable organo-mineral complexes of Al, Fe, and Mn (pyrophosphate extractable complexes ($\sum$Al, Fe, Mn)), sum of oxalate extractable Al, Fe, and Mn oxides (oxalate extractable oxides ($\sum$Al, Fe, Mn)), clay content, silt content, the sum of exchangeable bases (Ca, Mg, K), C:N ratio, and soil depth. Clay content was highly correlated with the removed sum of dithionite–citrate–bicarbonate extractable Al, Fe, and Mn oxides (DCB extractable oxides ($\sum$Al, Fe, Mn)). The sum of exchangeable bases correlated highly with several other removed soil fertility proxies (soil pH, bray-P; Figure S1). Finally, the VIF-assessed geochemical variables were used as explanatory variables in multiple linear stepwise regression to explain differences in SOC variables. Relative importance analysis of each explanatory variable was used to assess their predictive power.

IBM SPSS Statistics 26 (IBM, 2019) was used for ANOVA. PCA, cluster analyses, VIF assessment, stepwise regressions, and relative importance analysis were realized using R 3.6.1 (R Core Team, 2020) using the R packages *Relaimpo* (Grömping, 2006) and *Factoextra* (Kassambara & Mundt, 2020). The significance level for all statistical analysis was set at $p < .05$.

3 | RESULTS

3.1 | Geochemical dataset structure

The principal component analyses resulted in two distinct principal components (PCs; Figure 2a). PC 1 explains 64.8% variability in the data with significant positive loadings of total P (0.99) and TRB (0.99) and was thus interpreted as the axis representing "soil fertility." PC 2 explains 33.8% variability in the data with significant loadings of the sum of total metal concentration of Al, Fe, and Mn and was thus interpreted as the axis for "mineral C stabilization potential." The following cluster analyses yielded three distinct clusters based on TRB, total P, and total metal concentrations (Figure 2b,c) which roughly followed the investigated geochemical regions *mafic*, *felsic*, and *mixed sedimentary* as the main divide for structuring the data. The first cluster reflects geochemistry with low fertility and low mineral C stabilization potential. It contains 36 samples from both land use types and all geochemical regions but is dominated by samples from the mixed sedimentary region. The second cluster represents low fertility but high mineral C stabilization potential. This cluster contains 27 samples from both land use types of the mafic region. The third cluster represents high fertility and low mineral C stabilization potential. This cluster contains 19 samples from croplands of the felsic region and no forest samples.

The lack of forest sites in this cluster is explained through the preferential use of fertile land for cropping in an otherwise less fertile tropical soil landscape with deeply weathered soils (Ordway et al., 2017). An overview of ranges of soil properties grouped by the identified clusters are given in Table 3. Note that clay content was also identified to correlate with both soil fertility (Kome et al., 2019) and mineral C stabilization (Quesada et al., 2020). Here, due to this mixed role, it is hard to interpret its mechanistic role clearly, and we thus excluded it from informing the cluster formation (Figure 2a).

3.2 | SOC stocks and Δ^{14}C across land use and geochemical regions

3.2.1 | SOC stocks

Across geochemical clusters, no significant difference was found between land use types in means of SOC stocks for the upper meter of soil for any depth increment, except for an insignificant trend of higher SOC stocks in topsoils (0–10 cm) under forest in the low fertility/high stabilization potential cluster (Figure 3). Across both land uses, in the low fertility/high stabilization potential cluster, depth-explicit SOC stocks ranged from 43.6 ± 15.3 t C ha^{-1} at the soil surface (0–10 cm) to 15.3 ± 8.3 t C ha^{-1} in subsoil (90–100 cm). In the low fertility/low stabilization potential cluster, SOC stocks range from 40.8 ± 11.7 t C ha^{-1} at the soil surface to 18.9 ± 11.7 t C ha^{-1} in subsoil. In the high fertility/low stabilization cluster, SOC stocks range from 46.4 ± 11.0 t C ha^{-1} at the soil surface to 17.2 ± 4.6 t C ha^{-1} in subsoil.

Similarly, no significant differences in SOC stocks across geochemical clusters were detected under forest (Figure 3a) and cropland. SOC stocks ranged from 52.5 ± 17.6 t C ha^{-1} in topsoil (highest in forest) to 13.3 ± 9.3 t C ha^{-1} in subsoil (lowest in cropland).

3.2.2 | Soil Δ^{14}C

Differences in bulk soil Δ^{14}C across land use types were nonsignificant and no patterns with depth could be observed, except for higher soil Δ^{14}C in topsoil (0–30 cm) versus low values in subsoil (30–100 cm). However, soil Δ^{14}C for specific depth layers were significantly different when analyzing the data across geochemical clusters.

When comparing soil Δ^{14}C across geochemical clusters for each land use separately, differences were more pronounced between geochemical clusters under forest compared to cropland (Figure 3b). Under forest, the low fertility/low stabilization potential cluster (-86.0 ± 234.8‰ to -357.8 ± 80.6‰) shows lower soil Δ^{14}C signatures compared to the low fertility/high stabilization potential cluster ($+72.9 \pm 101.8$‰ to -290.0 ± 56.0‰). This difference was significant for the 40–50, 50–60, 70–80, and 80–90 cm depth increments. Under cropland, the high fertility/low stabilization potential cluster shows significantly higher soil Δ^{14}C signatures in the 0–10 cm ($+51.0\% \pm 53.1$‰) and lower values in the 90–100 cm depth increment (-399.0 ± 121.0‰) compared to both other clusters (Figure 3b).
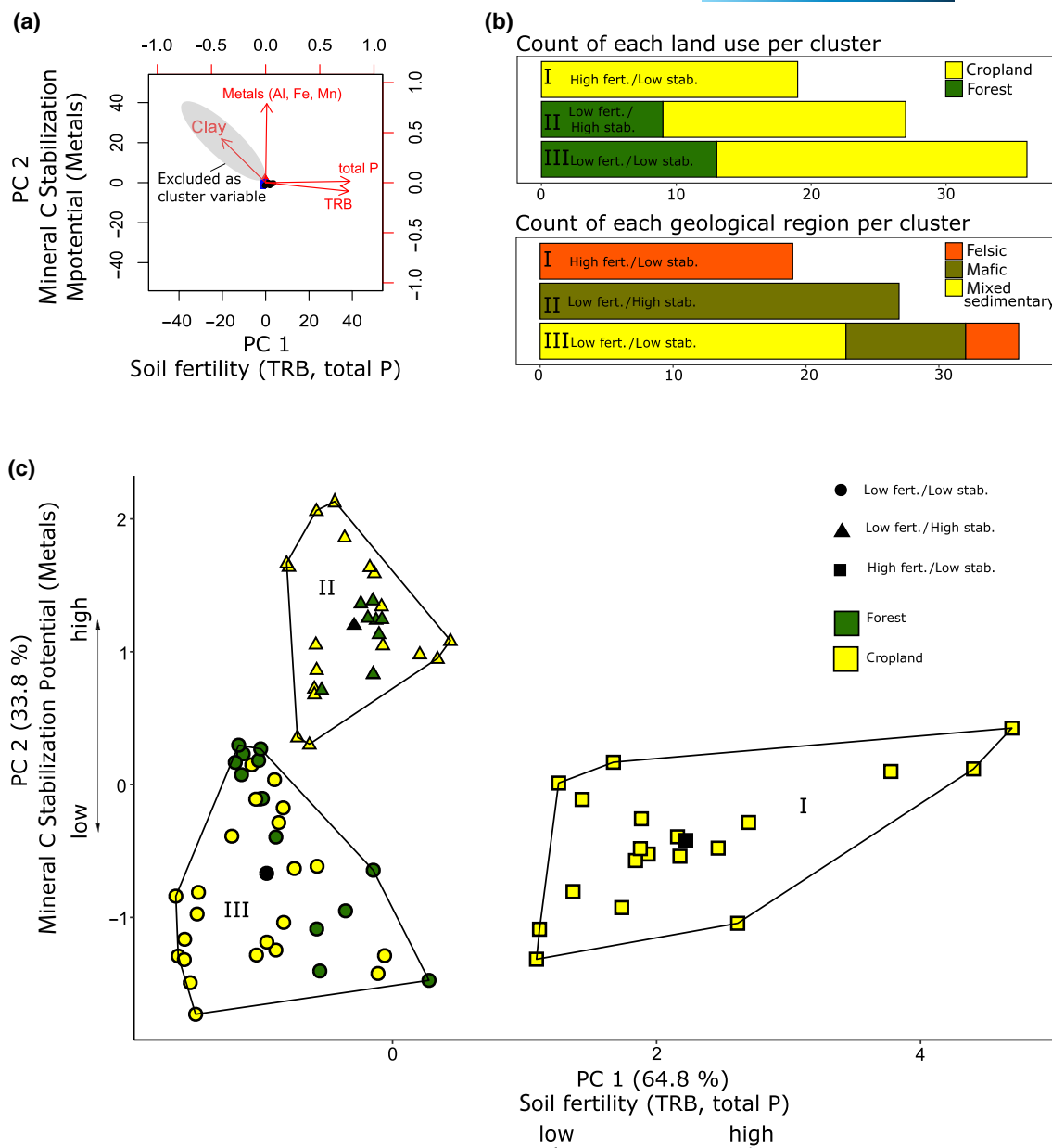
FIGURE 2 Cluster analysis considering TRB, total P, and the sum of total Al, Fe, and Mn concentrations of deeper subsoil samples (70–80, 80–90, and 90–100 cm; $n = 82$). Panel (a) Principal components that structure the dataset. Note the mixed role of clay, which was consecutively excluded to build clusters. Panel (b) Loading of clusters concerning data from varying land use and geochemical regions. Panel (c) Outcome of the K-mean clustering, resulting in three distinct clusters with respect to pairing of soil fertility and mineral C stabilization potential. The black symbol in each cluster shows the center point. Note that available rock-derived nutrients and pedogenic metal phases generally followed the same patterns as outlined here for total concentrations of rock-derived elements.

3.3 | Geochemical drivers of SOC stocks and soil $\Delta^{14}C$

3.3.1 | Predictors for SOC stocks

Based on the stepwise regression analysis, the included soil geochemical properties and soil depth explained between 71% and 90% of the variance in SOC stocks across land use types and geochemical clusters (Figure 4). While the structure of the regression models for cropland and forest was similar, model structures

differed significantly between geochemical clusters. The most important predictors across all clusters were pyrophosphate extractable organo-mineral complexes ($\sum$Al, Fe, Mn), which explained nearly half of the variance when using samples from both land use types and geochemical clusters combined. However, the importance of the latter reduced from 55% in the low fertility/low stabilization potential cluster to 32% in the high fertility/low stabilization potential cluster. The importance of soil depth remained fairly constant (19%–32%). Exchangeable base cations (Ca, Mg, K) were identified as a secondary control with prediction power
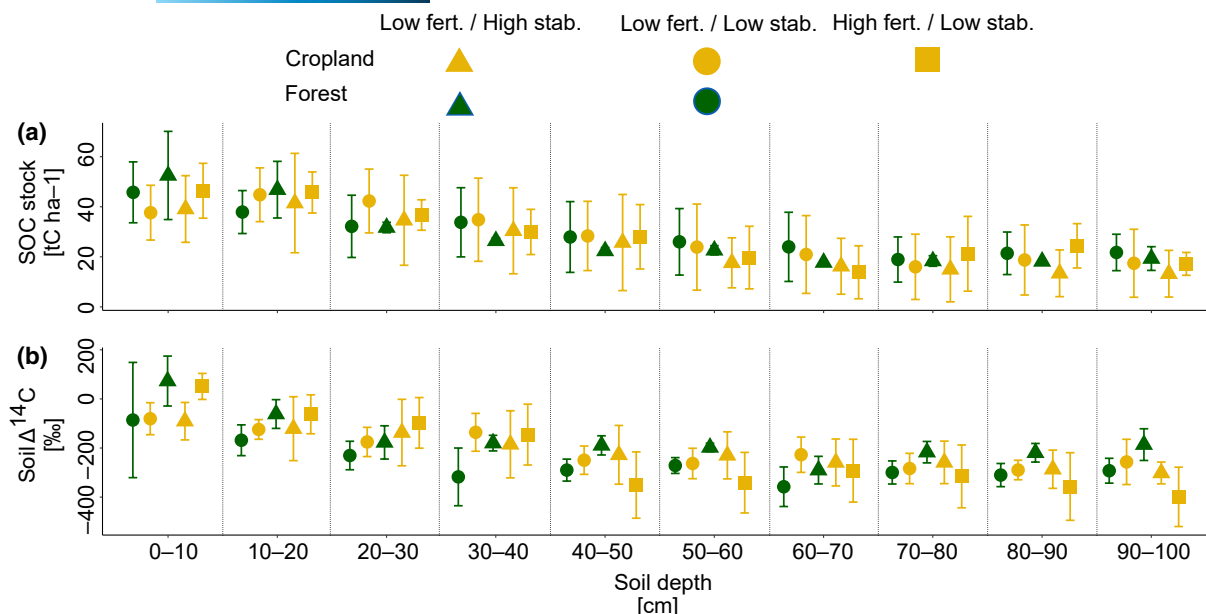
FIGURE 3 Comparison of (a) SOC stocks and (b) soil Δ^{14}C across land use types and geochemical clusters ($n = 3$–8). Symbols show means and error bars represent standard deviation. Where not visible, standard deviation bars were smaller than the symbol of the means. fert, soil fertility; stab, mineral stabilization potential.
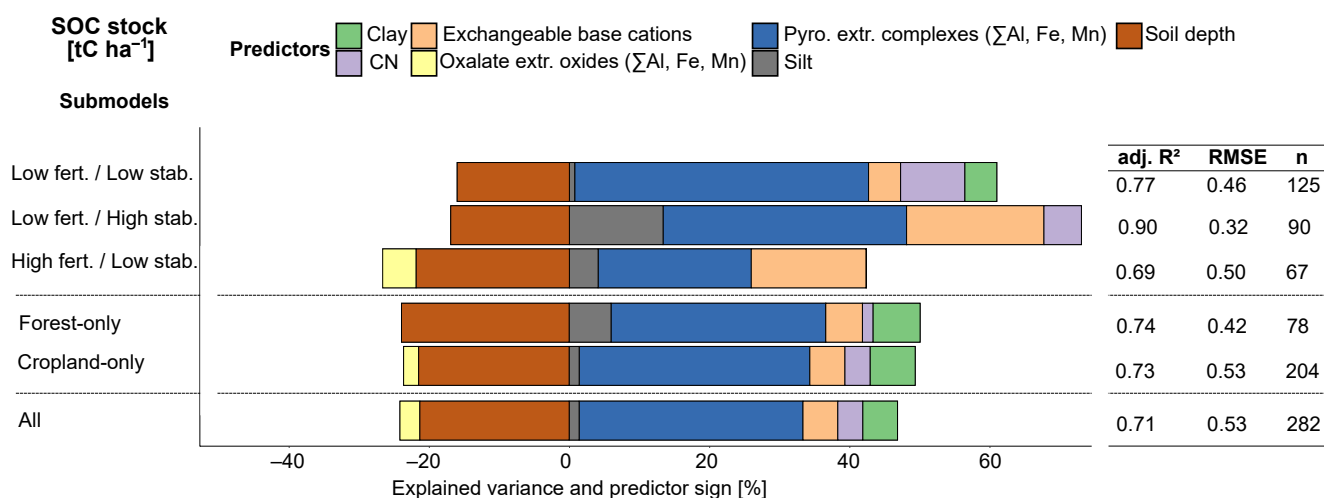

FIGURE 4 Regression analysis between SOC stocks and soil variables with relative importance and explained variance of predictors using observations from all increments until 1 m soil depth for different submodels (selected by geochemical cluster or land use) and all data points. Adjusted R^2 displays the goodness of fit. Root mean square error (RMSE) assesses the model quality. The length of the total bar for each plots represent the adj. R^2. The length of the colored sections in each plot represents the relative importance [%] of a respective explanatory variable, normalized to the adj. R^2. fert, soil fertility; stab, mineral stabilization potential.

ranging from 6% to 24% and were particularly important for the low fertility/high stabilization potential cluster and high fertility/low stabilization potential cluster. Silt and clay content ranked as tertiary controls between 1% and 15%, with higher predictive power for silt (6%–18%) only in the low fertility/high stabilization potential cluster and high fertility/low stabilization potential cluster. SOM quality (C:N ratio) contributed as a minor control, between 2% and 12%, on the explanatory power of the different models. Similarly, in contrast to the importance of pyrophosphate extractable organo-mineral complexes ($\sum$Al, Fe, Mn), oxalate extractable

oxides—extracted sequentially after using pyrophosphate—were of only minor importance (3%–7%).

3.3.2 | Predictors for soil Δ^{14}C patterns

The same set of predictors used for predicting SOC stocks explained between 45% and 81% of variance in soil Δ^{14}C across land use types and geochemical clusters (Figure 5). The explanatory power of models built for specific geochemical clusters was
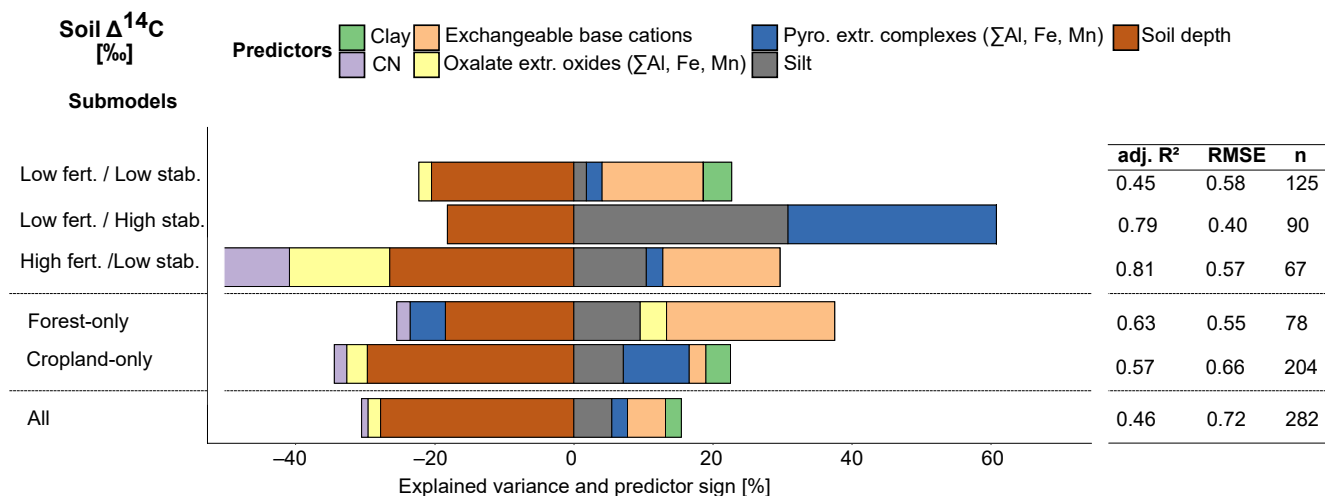
FIGURE 5 Regression analysis between soil $\Delta^{14}C$ and soil variables with relative importance and explained variance of predictors using observations from all increments to 1 m soil depth for different submodels (selected by geochemical cluster or land use) and all data points. Adjusted R^2 displays the goodness of fit. Root mean square error (RMSE) assesses the model quality. The length of the total bar for each plots represent the adj. R^2. The length of the colored sections in each plot represents the relative importance [%] of a respective explanatory variable, normalized to the adj. R^2. fert, soil fertility; stab, mineral stabilization potential.

generally similar or slightly higher (45%–81% of total explained variance) than the explanatory power of land use type differentiated models (57%–63% of total explained variance). However, the explanatory power over all data points was lower (46% of explained variance) compared to most of the submodels. Model structures across land use types were similar but with a generally lower importance of geochemical soil variables (3%–39%) than of soil depth (23%–61%), particularly in cropland. An exception was observed for exchangeable bases being more important in forest (38%) than soil depth (29%). Among the included soil variables and in contrast to the predictions of the SOC stocks, pyrophosphate extractable organo-mineral complexes ($\sum Al$, Fe, Mn) and oxalate extractable oxides ($\sum Al$, Fe, Mn) were ranked at the same importance (3%–38%) as soil texture (4%–39%). Included proxies for soil fertility (exchangeable base cations, 7%–38%), were important in both high and low fertility clusters. As observed in the SOC stock models, soil organic matter quality (C:N ratio) was also of minor importance across all soil $\Delta^{14}C$ models (2%–13%), with highest predictive power in the high fertility/low stabilization cluster. Notably, while overall important, soil depth was the weakest explanatory variable in the cluster with low fertility/high stabilization potential.

4 | DISCUSSION

4.1 | Data representativeness and caveats

4.1.1 | Spectroscopy and landforms

Our dataset ($n = 282$) represents a wide range of geochemical soil conditions including different land uses (forest, cropland) that were predicted using novel NIR-MIR spectrometry methods across a wide range of soil types with distinct properties. High variance

in the SOC data (Figure 3) is therefore not an artifact caused by our statistical approach but reflects the natural variability in a highly complex soil landscape. In agreement with other large-scale environmental data analyses (Baumann et al., 2021; Summerauer et al., 2021) an R^2 of .93 is to be considered very good in terms of spectroscopic estimates for predicting SOC. Similarly, the spectroscopic estimates of the geochemical predictor variables (Table 2) are considered to be good to very good compared to other studies (Baumann et al., 2021). Thus, the data quality and robustness of our SOC and geochemical data as well as its sample size enables us to interpret correlations across a variety of tropical soil and environmental conditions.

Similarly, an R^2 of .69 is sufficient to identify broad trends of soil $\Delta^{14}C$ across our regional-scale dataset. This indirect application of FT-IR spectroscopy to estimate soil $\Delta^{14}C$ is possible due to the availability of calibration data representing the range of environmental conditions (parent material, land use) within a spatially limited study region (Trumbore, 2009). However, several factors can affect soil $\Delta^{14}C$ besides measurable soil conditions and therefore, extrapolation of spectroscopic estimates of soil $\Delta^{14}C$ across larger spatial scales is not possible with the applied method. Additionally, note that the lowest model performance for explaining $\Delta^{14}C$ is in the low fertility/low stabilization potential cluster (Figure 5). This cluster contains samples with geogenic fossil organic carbon (Reichenbach et al., 2021). However, since the spectroscopic models are not calibrated for geogenic, fossil organic carbon, the estimated depth distribution is not able to identify their presence or absence. Note also that, since we focused on stable, non-eroding landforms, only the direct effects on SOC of land conversion and the pedogenetic variation of soil profiles along geochemical gradients were investigated. Effects of soil relocation through erosion and deposition would lead to substantial additional alteration of the soil C cycle (Doetterl et al., 2016) and is the subject of future work.

4.1.2 | Climatic variation

Overall, like many other field studies in underrepresented regions of the Tropics, our analysis lacks long-term data on differences in climatic factors affecting SOC stocks and soil Δ^{14}C, and measurements of site specific precipitation, soil moisture, and temperature dynamics would provide helpful additional insights. The coarser resolved global climate data available for the region (MAP, MAT, PET; Fick & Hijmans, 2017) is associated with substantial errors at the level of individual raster cells (Beck et al., 2020). However, given this range, estimates regarding the importance of climatic variables for analyses on SOC stocks and dynamics across land use and geochemistry are possible. Overall, we assume that climatic differences between study sites do not have a substantial effect on SOC dynamics. While one would expect forest soils to be generally cooler than cultivated soils due to the removal of the shading canopy, changes in C cycling due to soil temperature profiles between forests and croplands are likely limited to topsoils (Tian et al., 2017) and litter layers (not considered here). In addition, with the exception of the forest sites in the mafic region (ΔMAT to highest: −3.7°C), differences in MAT between the sites are relatively small (with a total range of 15.5–19.2°C). In the case of MAP, all forest sites have higher rainfall than the respective cropland site in each geochemical region (differences between study regions ranging from 192 to 322 mm, totals of 1465–1928 mm y^{-1}) with similar values in PET (1124–1486 mm y^{-1}). Taking into account the observed difference in MAT and MAP and the fact that tropical rainforests have a substantial interception potential (Rosalem et al., 2019), the slightly higher rainfall amount seems not to have substantially affected soil moisture or temperature conditions enough to strongly alter SOC dynamics. Otherwise, the lower MAT and higher MAP values in forest compared to cropland should lead to higher SOC stocks (Wagai et al., 2008), which we did not observe.

4.2 | Responses of SOC stocks and turnover across land use

Meta-analysis studies covering (tropical) soils across all continents recognize land conversion as a major driver of SOC stock changes both in top- and subsoils from primary forest to cropland (Don et al., 2011). In our study across distinct geochemical regions and focusing on deeply weathered and developed (non-eroded) soils, no effect of land conversion from forest to cropland on SOC stocks and soil Δ^{14}C could be detected, neither in topsoil nor in subsoil layers (Figure 3). To explain this observation, we argue that our findings point toward a limitation of C storage in deeply weathered soils that is independent of C inputs, which differ significantly between tropical forests and cropland (Bukombe et al., 2022; Kaiser et al., 2016). Rather, soil C storage seems to depend more strongly on a soil's ability to stabilize C inputs with the mineral matrix. In temperate soils of intermediate weathering stages, which are usually characterized by an abundance of highly reactive minerals that can sorb C, the soil (mineral) matrix

allows for stabilizing larger amounts of C over longer timescales in aerated (not water-logged) soils (Doetterl et al., 2018; Eusterhues et al., 2003; Torn et al., 1997). There, organo-mineral association can form stable complexes that represent an effective energetic barrier against microbial decomposition of organic matter. In the deeply weathered tropical soils investigated in our study, minerals have lost a significant amount of their reactivity toward C sorption during their long development history (Coward et al., 2017). Accordingly, labile pyrophosphate extractable complexes were far more important than the more commonly assessed oxalate extractable pedogenic oxides or soil clay content (Figure 4). Pyrophosphate extractable organo-mineral complexes can be attached to larger minerals (Wagai et al., 2020), but are usually interpreted as only weak agents for stabilizing C against microbial decomposition (Heckman et al., 2018; Lawrence et al., 2015; Paul et al., 2008). Thus, the C associated with them represents an easily available pool of C for microorganisms (Bukombe et al., 2021; Heckman et al., 2009). Overall, this means that organic matter cannot be efficiently stabilized in these soils and is more easily decomposed by microbial communities, leading to the observed limited differences in SOC stocks across land use with very different C inputs. Our data support this interpretation in several ways.

First, despite differences in C input and rooting patterns across geochemical regions in our study (Bukombe et al., 2022; Doetterl, Asifiwe, et al., 2021), SOC depth curves are similar between forest and cropland soils (Figure 3a, Figure S2). Importantly, the identified relationships between predictor variables and SOC content or soil Δ^{14}C do not change with soil depth or for separate depth increments (Table S2). Moreover, SOC stocks and soil Δ^{14}C show only weak depth trends due to sharp differences between top- and subsoil (Figure S2). This finding may be indicative of some disconnection between fast cycling C in topsoil versus C cycling in subsoil with slower turnover times. Second, soil Δ^{14}C patterns and the derived turnover time estimates for SOC at greater depths are still rather short compared to temperate soil systems and geochemically less altered (more reactive) soil systems in the (sub)tropics (Marín-Spiotta et al., 2008; Mathieu et al., 2015; Figure 3b). This indicates a shorter average turnover time of stored SOC in deeply weathered tropical soils compared to less weathered temperate soils, also at greater depth (Shi et al., 2020). The faster turnover of soil C at our study sites is also supported by results from laboratory incubations in recent studies conducted on samples from the same forest gradients as analyzed here. In these incubations, both top as well as subsoil C sources decomposed (Bukombe et al., 2021), and decomposer communities adapted their strategies to access nutrients according to specific nutrient limitations (Kidinda et al., 2022). Thus, mineral-bound organic matter may still sorb onto secondary minerals in deeply weathered soils, but Δ^{14}C data show that the turnover time of C remains short due to the limited ability to stabilize SOC in the long term because of the weakening of mineral-related protection of SOC against decomposition. Third, despite strong differences in pedogenic metal phases and clay content controlling mineral

C stabilization and the amount of rock-derived cations between geochemical regions (Doetterl, Asifiwe, et al., 2021; Reichenbach et al., 2021), only the (statistically) identified controls between geochemical clusters differed. SOC stocks and soil $\Delta^{14}C$ patterns remain similar (Figure 3–5).

Taken together, variations in controls on SOC dynamics between the investigated geochemical regions seem not to be strong enough to induce quantitative changes in SOC stocks and soil C turnover time in deeply weathered tropical soils. Consequently, efforts to increase soil carbon storage by improving land management and C inputs, or conversion of cropland into forests may only lead to limited responses in tropical SOC stocks in deeply weathered soils. Positive effects in terms of increasing SOC stocks by these measures might be restricted to the accumulation of labile organic matter in near surface horizons where they remain sensitive to future alterations in climate (Knorr et al., 2005; Wang et al., 2018) and land use (da Silva Oliveira et al., 2017; Sheng et al., 2015). Suggested efforts in this direction might therefore overestimate the potential increases in the C sink function of tropical soils that is achievable by reforestation, with positive effects limited to biomass C accumulation (Lewis et al., 2019; Silver et al., 2001, 2004).

5 | CONCLUSION AND OUTLOOK

We demonstrate that similar SOC stocks and SOC turnover times can be found in deeply weathered soils across tropical forest and cropland as well as geochemical regions. Differences in SOC dynamics between the investigated soils can be predicted predominantly by biogeochemical soil properties, and less by land use. Soils across geochemical regions differ in controls on SOC dynamics, but little in quantity of SOC and its distribution with soil depth. Across land use types and geochemical regions, a small selection of easy to measure soil mineral properties together with soil depth can explain between 69% and 90% of the variation in SOC stocks and between 46% and 81% of the variation in soil $\Delta^{14}C$ at the regional scale. The formation of labile organo-mineral complexes and the presence or absence of exchangeable base cations drive the observed variation in SOC stocks, but do not contribute to long-term SOC stability. In conclusion, the specific mineralogical properties and reactivity of tropical soils related to parent material and weathering status are an important factor to determine the potential impact that land conversion may or may not have on tropical soil C stocks. This information can help to guide efforts and identify regions where reforestation and the protection of intact plant–soil systems in the Tropics are most efficient, and where the potential to store more C in soils will be constrained by soil mineralogy.

AUTHOR CONTRIBUTIONS

Sebastian Doetterl and Peter Fiener designed the research. Mario Reichenbach conducted the sampling campaign and collected the data. All authors analyzed and interpreted the data. All authors contributed to the writing of the paper.

CONFLICT OF INTEREST STATEMENT

All authors declare that they have no conflict of interest.

DATA AVAILABILITY STATEMENT

The data that support the findings of this study are available in an open access project-specific database (Doetterl, Bukombe, et al., 2021) at https://doi.org/10.5880/fidgeo.2021.009.

SAMPLE AVAILABILITY

All physically remaining soil samples are logged and barcoded at the Department of Environmental Science at ETH Zurich, Switzerland.

ORCID

Mario Reichenbach https://orcid.org/0000-0002-4694-3579
Peter Fiener https://orcid.org/0000-0001-6244-4705
Alison Hoyt https://orcid.org/0000-0003-0813-5084
Susan Trumbore https://orcid.org/0000-0003-3885-6202
Johan Six https://orcid.org/0000-0001-9336-4185
Sebastian Doetterl https://orcid.org/0000-0002-0986-891X

REFERENCES

Amundson, R., Berhe, A. A., Hopmans, J. W., Olson, C., Sztein, A. E., & Sparks, D. L. (2015). Soil and human security in the 21st century. *Science*, *348*, 647. https://doi.org/10.1126/science.1261071

Augusto, L., Achat, D. L., Jonard, M., Vidal, D., & Ringeval, B. (2017). Soil parent material—A major driver of plant nutrient limitations in terrestrial ecosystems. *Global Change Biology*, *23*, 3808–3824. https://doi.org/10.1111/gcb.13691

Bailey, K., Lloyd, F., Kearns, S., Stoppa, F., Eby, N., & Woolley, A. (2005). Melilitite at Fort Portal, Uganda: Another dimension to the carbonate volcanism. *Lithos*, *85*, 15–25. https://doi.org/10.1016/j.lithos.2005.03.019

Barker, D. S., & Nixon, P. H. (1989). High-Ca, low-alkali carbonatite volcanism at Fort Portal, Uganda. *Contributions to Mineralogy and Petrology*, *103*, 166–177. https://doi.org/10.1007/BF00378502

Barré, P., Fernandez-Ugalde, O., Virto, I., Velde, B., & Chenu, C. (2014). Impact of phyllosilicate mineralogy on organic carbon stabilization in soils: Incomplete knowledge and exciting prospects. *Geoderma*, *235–236*, 382–395. https://doi.org/10.1016/j.geoderma.2014.07.029

Bascomb, C. L. (1968). Distribution of pyrophosphate-extractable iron and organic carbon in soils of various groups. *Journal of Soil Science*, *19*, 251–268. https://doi.org/10.1111/j.1365-2389.1968.tb01538.x

Baumann, P., Lee, J., Frossard, E., Schönholzer, L. P., Diby, L., Hgaza, V. K., Kiba, D. I., Sila, A., Sheperd, K., & Six, J. (2021). Estimation of soil properties with mid-infrared soil spectroscopy across yam production landscapes in West Africa. *Soil*, *7*, 717–731. https://doi.org/10.5194/soil-2020-100

Beck, E., Wood, E. F., McVicar, T. R., Zambrano-Bigiarini, M., Alvarez-Garreton, C., Baez-Villanueva, O. M., Sheffield, J., & Karger, D. N. (2020). Bias correction of global high-resolution precipitation climatologies using streamflow observations from 9372 catchments. *Journal of Climate*, *33*, 1299–1315. https://doi.org/10.1175/jcli-d-19-0332.s1

Beretta, A. N., Silbermann, A. V., Paladino, L., Torres, D., Bassahun, D., Mussell, R., & Garciá-Lamohte, A. (2014). Soil texture analysis using a hydrometer: Modification of the Bouyoucos method. *Ciencia e Investigación Agraria*, *42*, 263–271. https://doi.org/10.4067/S0718-16202014000200013

Besnard, S., Koirala, S., Santoro, M., Weber, U., Nelson, J., Gütter, J., Herault, B., Kassi, J., N'Guessan, A., Neigh, C., Poulter, B., Zhang, T., & Carvalhais, N. (2021). Mapping global forest age from forest inventories, biomass and climate data. *Earth System Science Data*, *13*, 4881–4896. https://doi.org/10.5194/essd-13-4881-2021

Black, C. A. (1965). *Method of soil analysis, part 2, chemical and microbiological properties*. American Society of Agronomy. https://doi.org/10.2134/agronmonogr9.2.2ed

Blake, G. R., & Hartge, K. H. (1986). Bulk density. In *SSSA book series: Methods of soil analysis. Part 1 physical and mineralogical methods* (p. 1188). https://doi.org/10.2136/sssabookser5.1.2ed.c13

Bouyoucos, G. J. (1962). Hydrometer method improved for making particle size analyses of soils. *Agronomy Journal*, *54*, 464–465. https://doi.org/10.2134/agronj1962.00021962005400050028x

Bruun, T. B., Elberling, B., & Christensen, B. T. (2010). Lability of soil organic carbon in tropical soils with different clay minerals. *Soil Biology and Biochemistry*, *42*, 888–895. https://doi.org/10.1016/j.soilbio.2010.01.009

Bukombe, B., Bauters, M., Boeckx, P., Cizungu, L., Cooper, M., Fiener, P., Kidinda, L. K., Makele, I., Muhindo, D. I., Rewald, B., Verheyen, K., & Doetterl, S. (2022). Soil geochemistry—And not topography—As a major driver of allocation, stocks and dynamics in forests and soils of African tropical montane ecosystems. *New Phytologist*, *236*, 1617–1690. https://doi.org/10.1111/nph.18469

Bukombe, B., Fiener, P., Hoyt, A. M., Kidinda, L. K., & Doetterl, S. (2021). Heterotrophic soil respiration and carbon cycling in geochemically distinct African tropical forest soils. *Soil*, *7*, 639–659. https://doi.org/10.5194/soil-7-639-2021

Cotrufo, M. F., Ranalli, M. G., Haddix, M. L., Six, J., & Lugato, E. (2019). Soil carbon storage informed by particulate and mineral-associated organic matter. *Nature Geoscience*, *12*, 989–994. https://doi.org/10.1038/s41561-019-0484-6

Coward, E. K., Thompson, A. T., & Plante, A. F. (2017). Iron-mediated mineralogical control of organic matter accumulation in tropical soils. *Geoderma*, *306*, 206–216. https://doi.org/10.1016/j.geoderma.2017.07.026

Crawley, M. J. (2009). *The R book* (p. 942). Wiley.

Curtis, P. G., Slay, C. M., Harris, N. L., Tyukavina, A., & Hansen, M. C. (2018). Classifying drivers of global forest loss. *Science*, *361*, 1108–1111. https://doi.org/10.1126/science.aau3445

Cusack, D. F., Chadwick, O. A., Ladefoged, T., & Vitousek, P. M. (2013). Long-term effects of agriculture on soil carbon pools and carbon chemistry along a Hawaiian environmental gradient. *Biogeochemistry*, *112*, 229–243. doi:10.1007/s10533-012-9718-z

da Silva Oliveira, D. M., Paustian, K., Cotrufo, M. F., Fjallos, A. R., Cerqeira, A. G., & Cerri, C. E. P. (2017). Assessing labile organic carbon in soils undergoing land use change in Brazil: A comparison of approaches. *Ecological Indicators*, *72*, 411–419. https://doi.org/10.1016/j.ecolind.2016.08.041

Dahlgren, R. A. (1994). Quantification of allophane and imogolite, quantitative methods in soil mineralogy. In J. E. Chais & J. W. Stucki (Eds.), *ASA, CSSA and SSSA Books (American Society of Agronomy, Crop Science Society of America, and Soil Science Society of America)* (pp. 430–451). Soil Science Society of America Journal.

Day, R. W., & Quinn, G. P. (1989). Comparisons of treatments after an analysis of variance in ecology. *Ecological Monographs*, *59*, 433–463. https://doi.org/10.2307/1943075

Degryze, S., Six, J., Paustian, K., Morris, S. J., Paul, E. A., & Merckx, R. (2004). Soil organic carbon pool changes following land-use conversions. *Global Change Biology*, *10*, 1120–1132. https://doi.org/10.1111/j.1365-2486.2004.00786.x

Dewitte, O., Jones, A., Spaargaren, O., Breuning-Madsen, H., Brossard, M., Dampha, A., Deckers, J., Gallali, T., Hallett, S., Jones, R., Kilasara, M., Le Roux, P., Michéli, E., Montanarella, L., Thiombiano, L., Van Ranst, E., Yemefack, M., & Zougmore, R. (2013). Harmonisation of the soil map of Africa at the continental scale. *Geoderma*, *211–212*, 138–153. https://doi.org/10.1016/j.geoderma.2013.07.007

Dick, D. P., Nunes Gonçalves, C., Dalmolin, R. S., Knicker, H., Klamt, E., Kögel-Knabner, I., Simões, M. L., & Martin-Neto, L. (2005). Characteristics of soil organic matter of different Brazilian Ferralsols under native vegetation as a function of soil depth. *Geoderma*, *124*, 319–333. https://doi.org/10.1016/j.geoderma.2004.05.008

Doetterl, D., Behre, A. A., Nadeu, E., Wang, Z., Sommer, M., & Fiener, P. (2016). Erosion, deposition and soil carbon: A review of process-level controls, experimental tools and models to adress C cycling in dynamic landscapes. *Earth-Science Reviews*, *154*, 102–122. https://doi.org/10.1016/j.earscirev.2015.12.005

Doetterl, S., Asifiwe, R. K., Baert, G., Bamba, F., Bauters, M., Boeckx, P., Bukombe, B., Cadisch, G., Cooper, M., Cizungu, L. N., Hoyt, A., Kabaseke, C., Kalbitz, K., Kidinda, L., Maier, A., Mainka, M., Mayrock, J., Muhindo, D., Mujinya, B. B., … Fiener, P. (2021). Organic matter cycling along geochemical, geomorphic, and disturbance gradients in forest and cropland of the African tropics—Project TropSOC database version 1.0. *Earth System Science Data*, *13*, 4133–4153. https://doi.org/10.5194/essd-13-4133-2021

Doetterl, S., Berhe, A. A., Arnold, C., Bodé, S., Fiener, P., Finke, P., Fuchslueger, L., Griepentrog, M., Harden, J. W., Nadeu, E., Schnecker, J., Six, J., Trumbore, S., van Oost, K., Vogel, C., & Boeckx, P. (2018). Links among warming, carbon and microbial dynamics mediated by soil mineral weathering. *Nature Geoscience*, *11*, 589–593. https://doi.org/10.1038/s41561-018-0168-7

Doetterl, S., Bukombe, B., Cooper, M., Kidinda, L., Muhindo, D., Reichenbach, M., Stegmann, A., Summerauer, L., Wilken, F., & Fiener, P. (2021). *TropSOC database, version 1.0. GFZ data services [data set]*. Helmholtz Centre Potsdam—GFZ German Research Centre for Geosciences Public Law Foundation. https://doi.org/10.5880/fidgeo.2021.009

Don, A., Schumacher, J., & Freibauer, A. (2011). Impact of tropical land use change on soil organic carbon stocks—A meta-analysis. *Global Change Biology*, *17*, 1658–1670. https://doi.org/10.1111/j.1365-2486.2010.02336.x

Dressée, P. L. C., & Lepersonne, J. (1949). *Carte Géologique 1.5000000*. Institut Royal Colonial Belge Commission centrale de látlas general du Congo Belge et du Ruanda-Urundi, Index No. 31.

Eby, G. N., Lloyd, F. E., & Woolley, A. R. (2009). Geochemistry and petrogenesis of the Fort Portal, Uganda, extrusive carbonatite. *Lithos*, *113*, 785–800. https://doi.org/10.1016/j.lithos.2009.07.010

Eusterhues, K., Rumpel, C., Kleber, M., & Kögel-Knabner, I. (2003). Stabilisation of soil organic matter by interactions with minerals as revealed by mineral dissolution and oxidative degradation. *Organic Geochemistry*, *34*, 1591–1600. https://doi.org/10.1016/j.orggeochem.2003.08.007

Fick, S. E., & Hijmans, R. J. (2017). WorldClim 2: New 1-km spatial resolution climate surfaces for global land areas. *International Journal of Climatology*, *37*, 4302–4315. https://doi.org/10.1002/joc.5086

Friedl, M. A., Sulla-Menashe, D., Tan, B., Schneider, A., Ramankutty, N., Sibley, A., & Huang, X. (2013). MODIS collection 5 global land cover: Algorithm refinements and characterization of new datasets. *Remote Sensing of Environment*, *114*, 168–182.

Fujisaki, K., Perrin, A.-S., Desjardins, T., Bernoux, M., Balbino, L. C., & Brossard, M. (2015). From forest to cropland and pasture systems: A critical review of soil organic carbon stocks changes in Amazonia. *Global Change Biology*, *21*, 2773–2786. https://doi.org/10.1111/gcb.12906

Gerland, P., Raftery, A. E., Ševčíková, H., Li, N., Gu, D., Spoorenberg, T., Alkema, L., Fosdick, B. K., Chunn, J., Lalic, N., Bay, G., Buettner, T., Heilig, G. K., & Wilmoth, J. (2014). World population stabilization unlikely this century. *Science*, *346*, 234–237. https://doi.org/10.1126/science.1257469

Gorelick, N., Hancher, M., Dixon, M., Ilyushchenko, S., Thau, D., & Moore, R. (2017). Google Earth Enginge: Planetary-scale geospatial analysis for everyone. *Remote Sensing of Environment*, *202*, 18–27. https://doi.org/10.1016/j.rse.2017.06.031

Gregorich, E., Greer, K., Anderson, D., & Liang, B. (1998). Carbon distribution and losses: Erosion and deposition effects. *Soil and Tillage Research*, *47*, 291–302. https://doi.org/10.1016/S0167-1987(98)00117-2

Grömping, U. (2006). Relative importance for linear regression in R: The package relaimpo. *Journal of Statistical Software*, *17*, 1–27. https://doi.org/10.18637/jss.v017.i01

Guillaume, T., Damris, M., & Kuzyakov, Y. (2015). Losses of soil carbon by converting tropical forest to plantations: Erosion and decomposition estimated by δ(13) C. *Global Change Biology*, *21*, 3548–3560. https://doi.org/10.1111/gcb.12907

Han, J., Kamber, M., & Pei, J. (2012). *Data mining: Concepts and techniques* (p. 703). Elsevier.

Heckman, K., Lawrence, C. R., & Harden, J. W. (2018). A sequential selective dissolution method to quantify storage and stability of organic carbon associated with Al and Fe hydroxide phases. *Geoderma*, *312*, 24–35. https://doi.org/10.1016/j.geoderma.2017.09.043

Heckman, K., Welty-Bernard, A., Rasmussen, C., & Schwartz, E. (2009). Geologic controls of soil carbon cycling and microbial dynamics in temperate conifer forests. *Chemical Geology*, *267*, 12–23. https://doi.org/10.1016/j.chemgeo.2009.01.004

Herold, N., Schöning, I., Michalzik, B., Trumbore, S., & Schrumpf, M. (2014). Controls on soil carbon storage and turnover in German landscapes. *Biogeochemistry*, *119*, 435–451. https://doi.org/10.1007/s10533-014-9978-x

Hossner, L. R. (1996). Dissolution of total elemental analysis. In *SSSA book series: Methods of soil analysis. Part 3. Chemical methods* (p. 1390). https://doi.org/10.2136/sssabookser5.3.c34

IBM. (2019). *IBM: SPSS statistics for windows*. IBM Corp.

Ito, A., & Wagai, R. (2017). Global distribution of clay-size minerals on land surface for biogeochemical and climatological studies. *Scientific Data*, *4*, 170103. https://doi.org/10.1038/sdata.2017.103

Kaiser, M., Zederer, D. P., Ellerbrock, R. H., Sommer, M., & Ludwig, B. (2016). Effects of mineral characteristics on content, composition, and stability of organic matter fractions separated from seven forest topsoils of different pedogenesis. *Geoderma*, *263*, 1–7. https://doi.org/10.1016/j.geoderma.2015.08.029

Kassambara, A., & Mundt, F. (2020). *Factoextra: Extract and visualize the results of multivariate analysis*. R Package Version 1.0.7. https://CRAN.R-project.org/package=factoextra

Kidinda, L. K., Olagoke, F. K., Vogel, C., Bukombe, B., Kalbitz, K., & Doetterl, S. (2022). Microbial properties in tropical montane forest soils developed from contrasting parent material—An incubation experiment. *Journal of Plant Nutrition and Soil Science*, *185*, 807–820. https://doi.org/10.1002/jpln.202100274

Kirsten, M., Mikutta, R., Vogel, C., Thompson, A., Mueller, C. W., Kimaro, D. N., Bergsma, H. L. T., Feger, K.-H., & Kalbitz, K. (2021). Iron oxides and aluminous clays selectively control soil carbon storage and stability in the humid tropics. *Scientific Reports*, *11*, 5076. https://doi.org/10.1038/s41598-021-84777-7

Knorr, W., Prentice, I. C., House, J. I., & Holland, E. A. (2005). Long-term sensitivity of soil carbon turnover to warming. *Nature*, *433*, 298–301. https://doi.org/10.1038/nature03226

Köchy, M., Hiederer, R., & Freibauer, A. (2015). Global distribution of soil organic carbon—Part 1: Masses and frequency distributions of SOC stocks for the tropics, permafrost regions, wetlands, and the world. *Soil*, *1*, 351–365. https://doi.org/10.5194/soil-1-351-2015

Kome, G. K., Enang, R. K., Tabi, F. O., & Yerima, B. P. K. (2019). Influence of clay minerals on some soil fertility attributes: A review. *Open Journal of Soil Science*, *9*, 155–188. https://doi.org/10.4236/ojss.2019.99010

Kramer, M. G., Sanderman, J., Chadwick, O. A., Chorover, J., & Vitousek, P. M. (2012). Long-term carbon storage through retention of dissolved aromatic acids by reactive particles in soil. *Global Change Biology*, *18*, 2594–2605. https://doi.org/10.1111/j.1365-2486.2012.02681.x

Lacrose, D. T. (2004). *Discovering knowledge in data. An introduction to data mining* (p. 222). John Wiley & Sons.

Lawrence, C. R., Harden, J. W., Xu, X., Schulz, M. S., & Trumbore, S. E. (2015). Long-term controls on soil organic carbon with depth and time: A case study from the Cowlitz River Chronosequence, WA USA. *Geoderma*, *247–248*. https://doi.org/10.1016/j.geoderma.2015.02.005

Lewis, T., Verstraten, L., Hogg, B., Wehr, B. J., Swift, S., Tindale, N., Menzies, N. W., Dalal, R. C., Bryant, P., Francis, B., & Smith, T. E. (2019). Reforestation of agricultural land in the tropics: The relative contribution of soil. Living biomass and debris pools to carbon sequestration. *Science of the Total Environment*, *649*, 1502–1513. https://doi.org/10.1016/j.scitotenv.2018.08.351

Lugato, E., Smith, P., Borrelli, P., Panagos, P., Ballabio, C., Orgiazzi, A., Fernandez-Ugalde, O., Montanarella, L., & Jones, A. (2018). Soil erosion is unlikely to drive a future carbon sink in Europe. *Science Advances*, *4*, eaau3523. https://doi.org/10.1126/sciadv.aau3523

Luo, X., Hou, E., Zhang, L., & Wen, D. (2020). Soil carbon dynamics in different types of subtropical forests as determined by density fractionation and stable isotope analysis. *Forest Ecology and Management*, *475*, 118401. https://doi.org/10.1016/j.foreco.2020.118401

Mangaza, L., Sonwa, D. J., Ebuy, G. B., Ebuy, J., & Kahindo, J.-M. (2021). Building a framework towards climate-smart agriculture in the Yangambi landscape, Democratic Republic of Congo (DRC). *International Journal of Climate Change Strategies and Management*, *13*, 320–338. https://doi.org/10.1108/IJCCSM-08-2020-0084

Marín-Spiotta, E., Swanston, C. W., Torn, M. S., Silver, W. L., & Burton, S. D. (2008). Chemical and mineral control of soil carbon turnover in abandoned tropical pastures. *Geoderma*, *143*, 49–62. https://doi.org/10.1016/j.geoderma.2007.10.001

Marthews, T. R., Riutta, T., Oliveras Menor, I., Urrutia, R., Moore, S., Metcalfe, D., Malhi, Y., Phillips, O., Huaraca Huasco, W., Ruiz Jaén, M., Girardin, C., Butt, N., Cain, R., & RAINFOR and GEM Networks. (2014). *Measuring tropical forest carbon allocation and cycling: A RAINFOR-GEM field manual for intensive census plots (v3.0). manual*. Global Ecosystems Monitoring Network. http://gem.tropicalforests.ox.ac.uk/

Mathieu, J. A., Hatté, C., Balesdent, J., & Parent, É. (2015). Deep soil carbon dynamics are driven more by soil type than by climate: A worldwide meta-analysis of radiocarbon profiles. *Global Change Biology*, *21*, 4278–4292. https://doi.org/10.1111/gcb.13012

McNally, S. R., Beare, M. H., Curtin, D., Meenken, E. D., Kelliher, F. M., Calvelo Pereira, R., Shen, Q., & Baldock, J. (2017). Soil carbon sequestration potential of permanent pasture and continuous cropping soils in New Zealand. *Global Change Biology*, *23*, 4544–4555. https://doi.org/10.1111/gcb.13720

Mehra, O. P., & Jackson, M. L. (1960). Iron oxide removal from soils and clays by a dithionite-citrate system buffered with sodium bicarbonate. *Clays and Clay Minerals*, *7*, 317–327. https://doi.org/10.1346/CCMN.1958.0070122

Mendez, J. C., van Eynde, E., Hiemstra, T., & Comans, R. N. (2022). Surface reactivity of the natural metal (hydr)oxides in weathered tropical soils. *Geoderma*, *406*, 115517. https://doi.org/10.1016/j.geoderma.2021.115517

Mikutta, R., Schaumann, G. E., Gildemeister, D., Bonneville, S., Kramer, M. G., Chorover, J., Chadwick, O. A., & Guggenberger, G. (2009). Biogeochemistry of mineral–organic associations across a long-term mineralogical soil gradient (0.3–4100 kyr), Hawaiian islands. *Geochimica et Cosmochimica Acta*, *73*, 2034–2060. https://doi.org/10.1016/j.gca.2008.12.028

Moder, K. (2007). How to keep the type I error rate in ANOVA if variances are heteroscedastic. *Austrian Journal of Statistics*, *36*, 179–188. https://doi.org/10.17713/ajs.v36i3.329

Nelson, D. W., & Sommers, L. E. (1996). Total carbon, organic carbon, and organic matter. In *SSSA book series: Methods of soil analysis. Part 3 chemical methods* (p. 1390). https://doi.org/10.2136/sssabookser5.3.c34

Okalebo, J. R., Gathua, K. W., & Woomer, P. L. (2002). *Laboratory methods of soil and plant analysis: A working manual* (4th ed., p. 131). SACRED Africa, Nairobi Office.

Ordway, E. M., Asner, G. P., & Lambin, E. F. (2017). Deforestation risk due to commodity crop expansion in sub-Saharan Africa. *Environmental Research Letters*, *12*, 44015. https://doi.org/10.1088/1748-9326/aa6509

Paul, S., Flessa, H., Veldkamp, E., & López-Ulloa, M. (2008). Stabilization of recent soil carbon in the humid tropics following land use changes: Evidence from aggregate fractionation and stable isotope analysis. *Biogeochemistry*, *87*, 247–263. https://doi.org/10.1007/s10533-008-9182-y

Pauwels, J. M., van Ranst, E., & Verloo, M. (1992). *Manuel de laboratoire de pédologie: Methods d'analyse de sols et de plantes, équipement, gestion de stocks de verrerie et de produits chimiques.* Centre universitaire de Dschang, Department des sciences du sol.

Perrin, A.-S., Fujisaki, K., Petitjean, C., Sarrazin, M., Godet, M., Garric, B., Horth, J.-C., Balbino, L. C., Filho, A. S., de Almeida Machado, P. L. O., & Brossard, M. (2014). Conversion of forest to agriculture in Amazonia with the chop-and-mulch method: Does it improve the soil carbon stock? *Agriculture, Ecosystems & Environment*, *184*, 101–114. https://doi.org/10.1016/j.agee.2013.11.009

Quesada, C. A., Paz, C., Oblitas Mendoza, E., Phillips, O. L., Saiz, G., & Lloyd, J. (2020). Variations in soil chemical and physical properties explain basin-wide Amazon forest soil carbon concentrations. *Soil*, *6*, 53–88. https://doi.org/10.5194/soil-6-53-2020

R Core Team. (2020). *A language and environment for statistical computing.* R Foundation for Statistical Computing. www.rstudio.com

Rasmussen, C., Heckman, K., Wieder, W. R., Keiluweit, M., Lawrence, C. R., Berhe, A. A., Blankinship, J. C., Crow, S. E., Druhan, J. L., Hicks Pries, C. E., Marin-Spiotta, E., Plante, A. F., Schädel, C., Schimel, J. P., Sierra, C. A., Thompson, A., & Wagai, R. (2018). Beyond clay: Towards an improved set of variables for predicting soil organic matter content. *Biogeochemistry*, *137*, 297–306. https://doi.org/10.1007/s10533-018-0424-3

Reichenbach, M., Fiener, P., Garland, G., Griepentrog, M., Six, J., & Doetterl, S. (2021). The role of geochemistry in organic carbon stabilization against microbial decomposition in tropical rainforest soils. *Soil*, *7*, 453–475. https://doi.org/10.5194/soil-7-453-2021

Rennert, T. (2019). Wet-chemical extractions to characterise pedogenic Al and Fe species—A critical review. *Soil Research*, *57*, 1. https://doi.org/10.1071/SR18299

Rosalem, L. M., Wendland, E. C., & Anache, J. A. (2019). Understanding the water dynamics on a tropical forest litter using a new device for interception measurement. *Ecohydrology*, *12*, e2058. https://doi.org/10.1002/eco.2058

Sanderman, J., & Chappell, A. (2013). Uncertainty in soil carbon accounting due to unrecognized soil erosion. *Global Change Biology*, *19*, 264–272. doi:10.1111/gcb.12030

Schimel, D., Pavlick, R., Fisher, J. B., Asner, G. P., Saatchi, S., Townsend, P., Miller, C., Frankenberg, C., Hibbard, K., & Cox, P. (2015). Observing terrestrial ecosystems and the carbon cycle from space. *Global Change Biology*, *21*, 1762–1776. https://doi.org/10.1111/gcb.12822

Senaviratna, N. A. M. R., & Cooray, T. M. J. A. (2019). Diagnosing multicollinearity of logistic regression model. *Asian Journal of Probability and Statistics*, *5*, 1–9. https://doi.org/10.9734/AJPAS/2019/v5i230132

Sheng, H., Zhou, P., Zhang, Y., Kuzyakov, Y., Zhou, Q., Ge, T., & Wang, C. (2015). Loss of labile organic carbon from subsoil due to land-use changes in subtropical China. *Soil Biology and Biochemistry*, *88*, 148–157. https://doi.org/10.1016/j.soilbio.2015.05.015

Shi, Z., Allison, S. D., He, Y., Levine, P. A., Hoyt, A. M., Beem-Miller, J., Zhu, Q., Wieder, W. R., Trumbore, S., & Randerson, J. T. (2020). The age distribution of global soil carbon inferred from radiocarbon measurements. *Nature Geoscience*, *13*, 555–559. https://doi.org/10.1038/s41561-020-0596-z

Silver, W. L., Kueppers, L. M., Lugo, A. E., Ostertag, R., & Matzek, V. (2004). Carbon sequestration and plant community dynamics following reforestation of tropical pasture. *Ecological Applications*, *14*, 1115–1127. https://doi.org/10.1890/03-5123

Silver, W. L., Ostertag, R., & Lugo, A. E. (2001). The potential for carbon sequestration through reforestation of abandoned tropical agricultural and pasture lands. *Restoration Ecology*, *8*, 394–407. https://doi.org/10.1046/j.1526-100x.2000.80054.x

Six, J., Conant, R. T., Paul, A., & Paustian, K. (2002). Stabilization mechanisms of soil organic matter: Implications for C-saturation of soils. *Plant Soil*, *241*, 155–176. https://doi.org/10.1023/A:1016125726789

Steinhof, A., Altenburg, M., & Machts, H. (2017). Sample preparation at the Jena 14C laboratory. *Radiocarbon*, *59*, 815–830. https://doi.org/10.1017/RDC.2017.50

Stucki, J. W., Goodman, B. A., & Schwertmann, U. (1988). *Iron in soils and clay minerals* (p. 894). Springer.

Stuiver, M., & Polach, A. H. (1977). Discussion reporting of 14C data. *Radiocarbon*, *19*, 355–363. https://doi.org/10.1017/S0033822200003672

Summerauer, L., Baumann, P., Ramirez-Lopez, L., Barthel, M., Bauters, M., Bukombe, B., Reichenbach, M., Boeckx, P., Kearsley, E., van Oost, K., Vanlauwe, B., Chiragaga, D., Heri-Kazi, A. B., Moonen, P., Sila, A., Shepherd, K., Mujinya, B. B., van Ranst, E., Baert, G., ... Six, J. (2021). Filling a key gap: A soil infrared library for Central Africa. *Soil*, *7*, 693–715. https://doi.org/10.5194/soil-7-693-2021

Tian, Q., Wang, X., Wang, D., Wang, M., Liao, C., Yang, X., & Liu, F. (2017). Decoupled linkage between soil carbon and nitrogen mineralization among soil depths in a subtropical mixed forest. *Soil Biology and Biochemistry*, *109*, 135–144. https://doi.org/10.1016/j.soilbio.2017.02.009

Torn, M. S., Trumbore, S. E., Chadwick, O. A., Vitousek, P. M., & Hendricks, D. M. (1997). Mineral control of soil organic carbon storage and turnover. *Nature*, *389*, 170–173. https://doi.org/10.1038/38260

Trumbore, S. (2009). Radiocarbon and soil carbon dynamics. *Annual Review of Earth and Planetary Sciences*, *37*, 47–66. https://doi.org/10.1146/annurev.earth.36.031207.124300

Tyukavina, A., Hansen, M. C., Potapov, P., Parker, D., Okpa, C., Stehman, S. V., Kommareddy, I., & Turubanova, S. (2018). Congo Basin forest loss dominated by increasing smallholder clearing. *Science Advances*, 4, eaat2993. https://doi.org/10.1126/sciadv.aat2993

Verdoodt, A., & Van Ranst, E. (2003). *Land evaluation for agricultural production in the tropics. A large-scale land suitability classification for Rwanda* (p. 183). Ghent University.

Vereecken, H., Schnepf, A., Hopmans, J. W., Javaux, M., Or, D., Roose, T., Vanderborght, J., Young, M. H., Amelung, W., Aitkenhead, M., Allison, S. D., Assouline, S., Baveye, P., Berli, M., Brüggemann, N., Finke, P., Flury, M., Gaiser, T., Govers, G., … Young, I. M. (2016). Modeling soil processes: Review, key challenges, and new perspectives. *Vadose Zone Journal*, 15, 1–57. https://doi.org/10.2136/vzj2015.09.0131

Vitousek, P. M., Porder, S., Houlton, B. Z., & Chadwick, O. (2010). Terrestrial phosphorus limitation: Mechanisms, implications, and nitrogen-phosphorus interactions. *Ecological applications*, 20, 5–15. https://doi.org/10.1890/08-0127.1

von Fromm, S. F., Hoyt, A. M., Lange, M., Acquah, G. E., Aynekulu, E., Berhe, A. A., Haefele, S. M., McGrath, S. P., Shepherd, K. D., Sila, A. M., Six, J., Towett, E. K., Trumbore, S. E., Vågen, T.-G., Weullow, E., Winowiecki, L. A., & Doetterl, S. (2021). Continental-scale controls on soil organic carbon across sub-Saharan Africa. *Soil*, 7, 305–332. https://doi.org/10.5194/soil-7-305-2021

Wagai, R., Kajiura, M., & Asano, M. (2020). Iron and aluminum association with microbially processed organic matter via meso-density aggregate formation across soils: Organo-metallic glue hypothesis. *Soil*, 6, 597–627. https://doi.org/10.5194/soil-6-597-2020

Wagai, R., Mayer, L. M., Kitayama, K., & Knicker, H. (2008). Climate and parent material controls on organic matter storage in surface soils: A three-pool, density-separation approach. *Geoderma*, 147, 23–33. https://doi.org/10.1016/j.geoderma.2008.07.010

Wang, Q., Zhao, X., Chen, L., Yang, Q., Chen, S., & Zhang, W. (2018). Global synthesis of temperature sensitivity of soil organic carbon decomposition: Latitudinal patterns and mechanisms. *Functional Ecology*, 33, 514–523. https://doi.org/10.1111/1365-2435.13256

Wei, X., Shao, M., Gale, W., & Li, L. (2014). Global pattern of soil carbon losses due to the conversion of forest to agricultural land. *Scientific Reports*, 4, 4062. https://doi.org/10.1038/srep04062

SUPPORTING INFORMATION

Additional supporting information can be found online in the Supporting Information section at the end of this article.